

Field- and Phage-Induced Dipolar Couplings in a Homodimeric DNA Quadruplex: Relative Orientation of G•(C–A) Triad and G-Tetrad Motifs and Direct Determination of C2 Symmetry Axis Orientation

Hashim M. Al-Hashimi,* Ananya Majumdar, Andrey Gorin, Abdelali Kettani, Eugene Skripkin, and Dinshaw J. Patel

Contribution from the Cellular Biochemistry and Biophysics Program, Memorial Sloan-Kettering Cancer Center, New York, New York 10021

Received September 14, 2000. Revised Manuscript Received November 16, 2000

Abstract: We present a new NMR procedure for determining the three-dimensional fold of C2-symmetric nucleic acid homodimers that relies on long-range orientational constraints derived from the measurement of two independent sets of residual dipolar couplings under two alignment conditions. The application is demonstrated on an $^{15}\text{N}/^{13}\text{C}$ -enriched deoxyoligonucleotide sequence, d(G-G-G-T-T-C-A-G-G), shown previously to dimerize into a quadruplex in solution and form a pair of G•(C-A) triads and G-G-G-G tetrads (G-tetrad) motifs. One-bond $^1\text{H}-^{15}\text{N}$ ($^1D_{\text{NH}}$) and $^1\text{H}-^{13}\text{C}$ ($^1D_{\text{CH}}$) residual dipolar couplings have been measured between nuclei in the bases of these motifs using bacteriophage as an ordering medium, and under direct magnetic field alignment (800 MHz). By combining the two dipolar data sets in an order matrix analysis, the orientation of the G•(C-A) triad relative to the G-tetrad within a contiguous monomeric unit can directly be determined, even in the presence of interstrand/intrastrand NOE ambiguity. We further demonstrate that the orientation of the C2-axis of molecular symmetry in the homodimer relative to the G•(C-A) triad and G-tetrad motifs can unambiguously be determined using the two sets of independent dipolar coupling measurements. The three-dimensional fold of the homodimer determined using this procedure is very regular and in excellent agreement with a previously determined high-resolution NOE-based NMR structure, where interstrand/intrastrand NOEs were treated as ambiguous and where noncrystallographic symmetry constraints were implicitly imposed during the structure calculation.

Introduction

It is now well established that DNA can adopt a wide range of multistranded architectures that go beyond the canonical Watson–Crick paired antiparallel double helix.¹ Higher-order DNA structures are of considerable interest because of their potential target for therapeutics² and because there is ample evidence that suggests such architectures may have specific functional roles in vivo.³ Many of these multistranded architectures are potential candidates for adaptation by DNA oligomers that contain elements of telomeric, centromeric, and triplet disease sequences.⁴ Structure determination of higher-order DNA structures at the duplex, triplex, and quadruplex level, is a critical step toward understanding the myriad recognition events that modulate DNA structure and function.

Nuclear magnetic resonance (NMR) spectroscopy is a powerful technique for determining bimolecular structure in the native solution state.⁵ However, as is the case for many proteins in vivo, many biologically relevant DNA folds adopt homomul-

timeric structures, and a number of limitations arise when applying the traditional NOE-based NMR approach to structure determination of higher-order multimers. One long-standing limitation is the inability to distinguish between inter- and intrastrand NOE cross-peaks.⁶ While techniques based on selective isotopic labeling of one domain have been developed to overcome this ambiguity problem in protein homodimers,^{7,8} they often cannot be applied to higher-order systems, and although one study has recently been reported,⁹ selective strand labeling is often prohibitively impractical for nucleic acids. Even under favorable circumstances where NOE ambiguities can be resolved, one must rely on what is often a small set of NOE-derived short distance constraints at monomeric interfaces in determining the overall structural organization of these monomeric units. For nucleic acid multimers, the low NOE density, the large number of degrees of freedom, and the extended molecular architecture further compounds these limitations. There have also been developments in structure refinement protocols that exploit the fact that homomultimers tend to aggregate symmetrically¹⁰ by implicitly imposing noncrystallographic symmetry constraints during the structure refinement.⁶

* To whom correspondence should be addressed. Telephone: (706) 639-7225. E-mail: hashimi@sbnmr1.mskcc.org.

(1) Neidle, S. *DNA Structure and Recognition*; Oxford University Press: Oxford, 1995.

(2) Kerwin, S. M. *Curr. Pharm. Des.* **2000**, *6*, 441–478.

(3) Rhodes, D.; Giraldo, R. *Curr. Opin. Struct. Biol.* **1995**, *5*, 311–322.

(4) Patel, D. J.; Bouaziz, S.; Kettani, A.; Wang, W. *Structures of Guanine-Rich and Cytosine-Rich Quadruplexes Formed in Vitro by Telomeric, Centromeric and Triplet Repeat Disease Sequences*; Oxford University Press: Oxford, 1999.

(5) Wüthrich, K. *NMR of Proteins and Nucleic Acids*; Wiley: New York, 1986.

(6) O'Donoghue, S.; Nilges, M. *Calculation of Symmetric Oligomer Structures from NMR Data*; Plenum: New York, 1999; Vol. 17.

(7) Folkers, P. J. M.; Folmer, R. H. A.; Konings, R. N. H.; Hilbers, C. W. *J. Am. Chem. Soc.* **1993**, *115*, 3798–3799.

(8) Folmer, R. H. A.; Hilbers, C. W.; Konings, R. N. H.; Hallenga, K. *J. Biomol. NMR* **1995**, *5*, 427–432.

(9) Kettani, A.; Bouaziz, S.; Skripkin, E.; Majumdar, A.; Wang, W.; Jones, R. A.; Patel, D. J. *Struct. Folding Des.* **1999**, *7*, 803–815.

(10) Weyl, H. *Symmetry*; Princeton University Press: Princeton, 1952.

However, a complementary source of long-range structural information that can directly overcome NOE ambiguity would be of significant and general utility.

Recently, developments in inducing weak levels of molecular alignment in high-resolution NMR applications have introduced residual dipolar couplings as a new source of structural information.^{11–14} Weak macromolecule alignment can be achieved directly under the influence of high magnetic fields when molecules have sufficiently large magnetic susceptibility anisotropies¹⁵ or more generally by dissolving molecules in ordered media, such as disc-shaped phospholipid bicelles^{13,16} and filamentous bacteriophage.^{17–19} Under these conditions, spectral resolution is retained while residual dipolar couplings are manifested as changes in the magnitude of normally observed scalar couplings.²⁰ The magnitude of residual dipolar couplings (D_{ij}) measured between two nuclei i and j is then given by

$$D_{ij} \propto \left\langle \frac{3 \cos^2 \theta - 1}{2r_{ij}^3} \right\rangle \quad (1)$$

where r is the internuclear distance, θ is the angle between the internuclear vector and the magnetic field, and the angle brackets denote a time average over all molecular orientations sampled by the internuclear vector.

Because of the angular dependence in eq 1, residual dipolar couplings measured between pairs of nuclei can be used to constrain the orientations of internuclear vectors relative to a common order tensor frame, and hence relative to one another, regardless of the distance separating internuclear vectors.¹⁴ Moreover, because dipolar couplings measured between bonded nuclei are intrinsically “intramonomeric”, derived orientational constraints can directly be used in the structure determination of contiguous monomeric units within multimers, even though intra- and intermonomer NOE contacts may be ambiguous. Even more significant is the fact that molecular symmetry, and more specifically, point group symmetry which arises in many multimeric structures,¹⁰ has a predetermined effect on partial molecular alignment, and this long-range structural information can be used to determine how monomeric units are organized in the multimer. These ramifications of molecular symmetry on molecular alignment have been known ever since the early liquid crystal NMR era in applications to small organic molecules²¹ and have recently been exploited in a ligand exchange study involving a homotrimer protein that has a C3-axis of molecular symmetry.²² Specifically, it was shown that the direction of principal order (S_{zz}) will always point along the C3-axis of symmetry, which allowed determination of ligand

bound geometry even in the absence of dipolar data on the protein itself.²³ Subsequently, Clore and co-workers used residual dipolar coupling measurements in conjunction with back calculation of dipolar couplings based on molecular shape to constrain the relative orientation of two monomers in a domain-swapped dimer having C2 symmetry.²⁴

While the utility of residual dipolar couplings has primarily focused on obtaining long-range orientational constraints in the structure determination of proteins,^{14,25} there are far fewer applications in the structure determination of nucleic acids. One preliminary study that has been reported involves structure determination of an RNA molecule complexed to a protein,²⁶ and very recently, a more extensive study appeared on an isolated DNA dodecamer molecule.²⁷ Here, we demonstrate an application in determining the three-dimensional fold of a C2-symmetric *homodimer* d(G-G-G-T-T-C-A-G-G) quadruplex (Figure 1a) that relies on an order matrix analysis of two independent sets of dipolar couplings measured using a bacteriophage medium as a source of molecular alignment and under direct magnetic field alignment. We demonstrate that the orientation of a G-(C-A) triad (Figure 1b) and a G-G-G-G tetrad (G-tetrad) (Figure 1c) motif, which were previously characterized by observation of NOEs and trans-hydrogen bond scalar couplings,^{28–30} may be determined unambiguously, both relative to one another within a contiguous monomeric unit and relative to their equivalent C2-symmetry related counterparts in the homodimer. The DNA topology calculated using this procedure is very regular and in excellent agreement with the previous NOE and hydrogen bond-based solution NMR structure.³⁰

Materials and Methods

Sample Preparation. Uniformly ¹³C/¹⁵N-labeled d(G-G-G-T-T-C-A-G-G) sequence was enzymatically synthesized using a modified version of the Zimmer and Crothers procedure³¹ as previously described.³⁰ Two samples were used to collect the residual dipolar couplings data, both of which contained 5% ²H₂O buffer (100 mM NaCl, 2 mM phosphate (pH 6.6)). One sample contained 2 mM ¹³C/¹⁵N uniformly labeled oligonucleotide (isotropic sample), while the second sample contained 0.8 mM ¹³C/¹⁵N uniformly labeled d(G-G-G-T-T-C-A-G-G) and 20 mg/mL Pf1 bacteriophage as an orienting medium (oriented sample). Pf1 bacteriophage was prepared as previously described.¹⁷ The NMR sample containing Pf1 bacteriophage and DNA was stable for over two years.

NMR Measurements. All NMR data were acquired at 20 °C on Varian Inova spectrometers operating at ¹H frequencies of 500, 600, and 800 MHz, equipped with 5 mm triple resonance, actively shielded, z-gradient probes. One-bond ¹H–¹³C splittings were measured in both samples at 500 MHz, and additionally at 800 MHz for the isotropic sample, using a frequency-based coupling enhanced, constant time ¹H–¹³C heteronuclear single quantum coherence (HSQC) experiment

(11) Bastiaan, E. W.; Maclean, C.; Van Zijl, P. C. M.; Bothner-by, A. A. *Ann. Rep. NMR. Spectrosc.* **1987**, *19*, 35–77.

(12) Tolman, J. R.; Flanagan, J. M.; Kennedy, M. A.; Prestegard, J. H. *Proc. Natl. Acad. Sci. U.S.A.* **1995**, *92*, 9279–9283.

(13) Tjandra, N.; Bax, A. *Science* **1997**, *278*, 1111–1114.

(14) Prestegard, J. H.; Al-Hashimi, H. M.; Tolman, J. R. *Q. Rev. Biophys.* **2000**, in press.

(15) Prestegard, J. H.; Tolman, J. R.; Al-Hashimi, H. M.; Andrec, M. In *Biological Magnetic Resonance*; Krishna, N. R., Berliner, L. J., Eds.; Plenum: New York, 1999; Vol. 17, pp 311–355.

(16) Sanders, C. R.; Schwonek, J. P. *Biochemistry* **1992**, *31*, 8898–8905.

(17) Hansen, M. R.; Mueller, L.; Pardi, A. *Nat. Struct. Biol.* **1998**, *5*, 1065–1074.

(18) Hansen, M. R.; Hanson, P.; Pardi, A. *Method Enzymol.* **2000**, *317*, 220–240.

(19) Clore, G. M.; Starich, M. R.; Gronenborn, A. M. *J. Am. Chem. Soc.* **1998**, *120*, 10571–10572.

(20) Bothner-By, A. A.; Domaille, P. J.; Gayathri, C. *J. Am. Chem. Soc.* **1981**, *103*, 5602–5603.

(21) Saupe, A. *Angew. Chem., Int. Ed. Engl.* **1968**, *7*, 97–112.

(22) Bolon, P. J.; Al-Hashimi, H. M.; Prestegard, J. H. *J. Mol. Biol.* **1999**, *293*, 107–115.

(23) Al-Hashimi, H. M.; Bolon, P. J.; Prestegard, J. H. *J. Magn. Reson.* **2000**, *142*, 153–158.

(24) Bewley, C. A.; Clore, G. M. *J. Am. Chem. Soc.* **2000**, *122*, 6009–6016.

(25) Delaglio, F.; Kontaxis, G.; Bax, A. *J. Am. Chem. Soc.* **2000**, *122*, 2142–2143.

(26) Bayer, P.; Varani, L.; Varani, G. *J. Biomol. NMR* **1999**, *14*, 149–155.

(27) Tjandra, N.; Tate, S.; Ono, A.; Kainosho, M.; Bax, A. *J. Am. Chem. Soc.* **2000**, *122*, 6190–6200.

(28) Dingley, A. J.; Grzesiek, S. *J. Am. Chem. Soc.* **1998**, *120*, 8293–8297.

(29) Pervushin, K.; Ono, A.; Fernandez, C.; Szyperski, T.; Kainosho, M.; Wuthrich, K. *Proc. Natl. Acad. Sci. U.S.A.* **1998**, *95*, 14147–14151.

(30) Kettani, A.; Basu, G.; Gorin, A.; Majumdar, A.; Skripkin, E.; Patel, D. J. *J. Mol. Biol.* **2000**, *301*, 129–146.

(31) Zimmer, D. P.; Crothers, D. M. *Proc. Natl. Acad. Sci. U.S.A.* **1995**, *92*, 3091–3095.

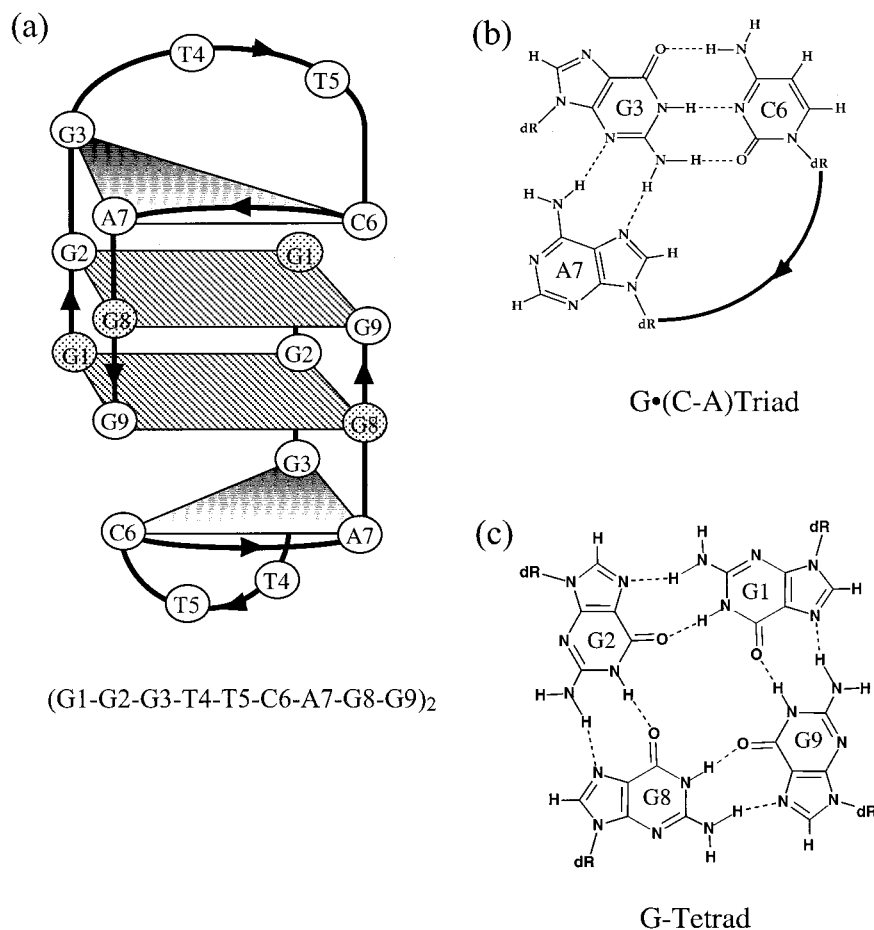


Figure 1. (a) Schematic showing the C₂-symmetric topology of the dimeric d(G-G-G-T-T-C-A-G-G) quadruplex as previously determined by NMR.³⁰ The two strands are related by a C₂-axis of symmetry that lies perpendicular to the normal of the base planes. G•(C-A) triad and G-tetrad structural motifs are shown as “dashed” rectangles and shaded triangles, respectively. (b) Base-paired alignment of the G3•(C6-A7) triad. (c) Base-paired alignment of the G1•G2•G8•G9 tetrad (G-tetrad).

($J_{\text{CH-CT-CE-HSQC}}$).³² This is a modified CT-HSQC experiment, which allows ^{13}C chemical shift to evolve for a period t_1 , and ^1H - ^{13}C couplings to evolve for a period $n \times t_1$, where n is an adjustable coupling enhancement factor. For all experiments, a coupling enhancement factor of 2 was used, resulting in a doubling of ^1H - ^{13}C splittings without an inherent increase in line width. Using a coupling enhancement scheme also helps reduce the potentially problematic effects of CSA/dipole-dipole cross-correlation. One-bond ^1H - ^{15}N splittings were measured in both samples at 500 MHz, and additionally at 800 MHz for the isotropic sample, also using a frequency-based coupling enhanced variation of the ^1H - ^{15}N heteronuclear single quantum coherence (HSQC) experiment (^1H - ^{15}N SCE-HSQC).³³ Acquisition parameters are listed in the legend of Table 1.

In all cases, splittings were extracted using a Bayesian time-domain NMR parameter estimation program Xrambo, using the method previously described.³⁴ Typically, the 2D matrix was processed only in the direct (ω_2) dimension, and an array of interferograms along the indirect dimension was used as input for the program. Typically, 4–16 interferograms for a given splitting were analyzed simultaneously. The following model was used for the data. Each component of the doublet was given an independent line width and intensity to allow for cross-correlated relaxation between chemical shift anisotropy (CSA) and dipole-dipole interactions. An independent phase was also used for each doublet to circumvent any phase problems arising from finite J -coupling evolution during the first t_1 point. Values for shifts, line

widths, phases, and intensities were estimated and entered as starting parameters which were subsequently refined by Xrambo's Metropolis Monte Carlo methods.³⁴ Splittings and associated random errors were obtained after convergence at a rejection rate of 60–65%. Phage-induced residual dipolar couplings were computed from the difference between splittings measured in the oriented and isotropic sample. Dipolar couplings calculated in this manner are devoid of any contribution from direct magnetic field alignment since both data sets were acquired at 500 MHz. Phage-induced dipolar couplings and associated uncertainties are shown in Table 1. Residual dipolar couplings at 800 MHz were computed using splittings measured at 500 and 800 MHz and using the quadratic field dependence (B^2) of dipolar couplings as previously described.¹² Field-induced dipolar couplings and associated uncertainties are also shown in Table 1.

Order Matrix Analysis. Order tensor calculations were carried out using the program ORDERTEN_SVD.³⁵ Coordinates for individual internuclear vectors in the G-tetrad and G•(C-A) triad were obtained from the NOE-based NMR structure (PDB 1fs3), and used as input for the program, along with corresponding residual dipolar coupling measurements and associated uncertainties (see Table 1). Input uncertainties for phage- and field-induced dipolar coupling measurements were set at $\sim 4.5\times$ and $\sim 3\times$ the uncertainty values shown in Table 1, to accommodate small departures in the assumed local geometry and internal motions.

The ORDERTEN_SVD program determines a set of allowed order tensor solutions by reiteratively selecting couplings from a normal distribution about the input values and solving the set of equations given in eq 2. Typically, 100 000 iterations were used. The program also

(32) Tian, F.; Al-Hashimi, H. M.; Craighead, J.; Prestegard, J. H. *J. Am. Chem. Soc.* **2000**, in press.

(33) Tolman, J. R.; Prestegard, J. H. *J. Magn. Reson., Ser. B* **1996**, *112*, 269–274.

(34) Andrec, M.; Prestegard, J. H. *J. Magn. Reson.* **1998**, *130*, 217–232.

(35) Losonczi, J. A.; Andrec, M.; Fischer, M. W. F.; Prestegard, J. H. *J. Magn. Reson.* **1999**, *138*, 334–342.

Table 1. $^1D_{CH}$ and $^1D_{NH}$ Residual Dipolar Couplings (RDC) and Uncertainties Measured in the Bases of the G•(C-A) and G-tetrad in the Dimeric d(G-G-G-T-T-C-A-G-G) Quadruplex

| vector ^a | phage-induced RDC (Hz) ^b | field-induced RDC (Hz) ^c |
|---------------------|-------------------------------------|-------------------------------------|
| G•(C-A) Triad | | |
| G3(N1H1) | 2.5 ± 0.2 | 0.5 ± 0.2 |
| G3(C8H8) | -1.7 ± 0.4 | -2.1 ± 0.4 |
| C6(C5H5) | 11.7 ± 1 | 1.6 ± 0.4 |
| C6(C6H6) | 14.3 ± 0.7 | -0.7 ± 0.3 |
| A7(C2H2) | 17.2 ± 0.4 | 0.2 ± 0.4 |
| A7(C8H8) | 21.1 ± 0.4 | 0.8 ± 0.9 |
| G-Tetrad | | |
| G1(N1H1) | -1.0 ± 0.2 | 1.1 ± 0.2 |
| G1(C8H8) | 3.9 ± 0.4 | -1.9 ± 0.2 |
| G2(N1H1) | -0.2 ± 0.2 | 1.0 ± 0.2 |
| G2(C8H8) | 0.0 ± 0.5 | -0.3 ± 0.4 |
| G8(N1H1) | -3.5 ± 0.2 | 1.0 ± 0.2 |
| G8(C8H8) | 12.7 ± 0.7 | -3.1 ± 0.2 |
| G9(N1H1) | -2.4 ± 0.2 | 1.0 ± 0.2 |
| G9(C8H8) | 0.2 ± 0.4 | -1.6 ± 0.4 |

^a Base internuclear vectors for which dipolar couplings were measured. All dipolar couplings were measured between directly bonded nuclei. ^b RDCs measured using a phage medium as a source for molecular alignment (phage-induced dipolar couplings). Dipolar couplings were computed from the differences in splittings measured in the oriented sample (J+D) and isotropic sample (J). ^c RDC measured under direct field alignment at 800 MHz (field-induced dipolar couplings). Field-induced RDCs were computed from the quadratic magnetic field dependence of splittings measured at 500 and 800 MHz. ^{b,c} One-bond $^1H-^{13}C$ splittings were measured using the $^1J_{CH-CT-CE-HSQC}$ experiment.³² Acquisition parameters at 500/800 MHz were: spectral width in the direct dimension (sw) = 7.0/8.5 kHz, and in the indirect dimension (sw1) = 2.0/6.033 kHz, number of complex data points in the direct dimension (np) = 544/768 (t_2^{max} = 77.6/124.8 ms), increments in the indirect dimension (ni) = 50/168 (t_1^{max} = 24.5/27.7 ms) and constant time delay (CT) = 28/56 ms. One-bond $^1H-^{15}N$ splittings were measured using the $^1H-^{15}N$ SCE-HSQC experiment.³³ The following acquisition parameters were used: at 500 MHz for the isotropic sample: sw = 8.5 kHz, sw1 = 1.5 kHz, np = 640 (t_2^{max} = 75.2 ms) and ni = 256 points (t_1^{max} = 170 ms). For the oriented sample at 500 MHz, all parameters were identical except sw1 = 900 Hz and ni = 128 (t_1^{max} = 141 ms). At 800 MHz for the isotropic sample: sw = 14.0 kHz, sw1 = 1.6 kHz, np = 1056 (t_2^{max} = 73.4 ms), ni = 256 points (t_1^{max} = 157 ms). Random uncertainties in frequency domain spectra were extracted using a Bayesian time-domain NMR parameter estimation program Xrambo.

diagonalizes the generated order matrices, and keeps only solutions that are consistent with the original input data. This procedure was carried out independently for the G•(C-A) triad and G-tetrad structural motifs using phage-induced dipolar couplings. The G•(C-A) triad and G-tetrad motifs were subsequently rotated into the independently determined principal axis system of phage-induced alignment, to yield four relative orientations that are consistent with phage-induced residual dipolar couplings, as previously described.^{35,36} Order tensor calculations were repeated for the G•(C-A) triad and G-tetrad in combination, independently for the four G•(C-A) triad/G-tetrad assemblies as input coordinates, and using field-induced dipolar couplings.

Results and Discussion

Order Matrix Analysis and C2 Symmetry. The order matrix approach that we employ in this study has been applied widely to protein systems and is particularly well suited for extracting orientational constraints from a small set of residual dipolar coupling measurements.^{21,35} Provided with the measurement of five or more independent residual dipolar couplings per known molecular fragment, one can solve for the five independent order matrix elements describing average fragment

alignment using eq 2

$$\left\langle \frac{3 \cos^2 \theta - 1}{2I_{ij}^3} \right\rangle = \sum_{ij=(x,y,z)} S_{ij} \cos \alpha_{ik} \cos \alpha_{jk} \quad (2)$$

³⁵ where S_{ij} are elements of a symmetric and traceless 3×3 order matrix, and α_{ik} is the angle between the k th internuclear vector and the i th axis of an arbitrarily chosen fragment coordinate frame. Diagonalizing the order matrix formed from these elements yields a transformation matrix (R), which can be used to assemble fragments into a structure by sequentially transforming chosen arbitrary fragment frames, into the common principal order tensor frame.³⁵ While a 4^{n-1} -fold degeneracy arises in the assembly of n molecular fragments due to allowed inversions about principal axes, this degeneracy can be overcome by acquiring two independent sets of residual dipolar couplings under different alignment conditions.³⁶

In application to protein systems, molecular fragments have varied from small peptide units,³⁷ to secondary structural elements,³⁸ to individual protein domains in multidomain systems.³⁹ For application to our target dimeric d(G-G-G-T-T-C-A-G-G) quadruplex, the G-tetrad and G•(C-A) triad structural motifs are a good choice for molecular fragments (Figure 1b and c).³⁰ First, determining the relative orientation of these motifs is of great interest, not only because this largely dictates the overall extended topology of this DNA molecule, but also because obtaining distance constraints on these relative orientations is complicated by inter- and intra strand NOE ambiguity. Second, structural characterization of these base-paired structural motifs is now generally and readily possible using trans-hydrogen bond scalar coupling experiments.^{9,30,40,41} Finally, because bases in these structural motifs are stabilized internally by hydrogen-bonding networks, they can be assumed to be relatively rigid, obviating the need to analyze dipolar couplings in regions where internal motions may be more extensive, for example, in ribose sugar rings.

Previous NMR stoichiometry studies indicate that the deoxyoligonucleotide sequence d(G-G-G-T-T-C-A-G-G) forms a dimeric architecture under the chosen NMR sample conditions.³⁰ This and the fact that only a single set of NMR resonances is observed are strong enough a priori evidence that the homodimer assumes a C2-symmetric topology¹⁰ (Figure 1a). In the presence of C2 molecular symmetry, one of the three principal axes of the order tensor will point along the C2-axis of symmetry.^{21,24} This information is of significant utility, since it can be used to relate the orientation of a given molecular fragment to its equivalent counterpart in the C2-symmetric homodimer. However, unlike C3 molecular symmetry,²³ C2 symmetry has no ramification on the order parameters S_{zz} and η describing extent and asymmetry of molecular alignment, and hence, it is generally not possible to uniquely establish which of the three principal axes corresponds to the C2-axis of molecular symmetry. Moreover, because there are no restrictions on the asymmetry parameter, η , the C2-axis of symmetry can also lie anywhere with equal probability in the principal $x-y$ plane of

(37) Tolman, J. R.; Al-Hashimi, H. M.; Kay, L. E.; Prestegard, J. H. *J. Am. Chem. Soc.* **2000**, in press.

(38) Fowler, C. A.; Tian, F.; Al-Hashimi, H. M.; Prestegard, J. H. *J. Mol. Biol.* **2000**, in press.

(39) Fischer, M. W. F.; Losonczi, J. A.; Weaver, J. L.; Prestegard, J. H. *Biochemistry* **1999**, *38*, 9013–9022.

(40) Majumdar, A.; Kettani, A.; Skripkin, E.; Patel, D. J. *J. Biomol. NMR* **1999**, *15*, 207–211.

(41) Kettani, A.; Gorin, A.; Majumdar, A.; Hermann, T.; Skripkin, E.; Zhao, H.; Jones, R.; Patel, D. J. *J. Mol. Biol.* **2000**, *297*, 627–644.

(36) Al-Hashimi, H. M.; Valafar, H.; Terrell, M.; Zartler, E. R.; Eidsness, M. K.; Prestegard, J. H. *J. Magn. Reson.* **2000**, *143*, 402–406.

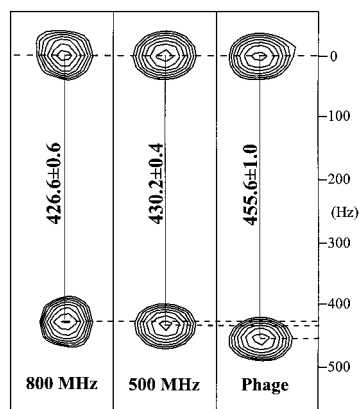


Figure 2. Representative spectra for ^1H – ^{13}C splittings between C8H8 nuclei in residue G8 acquired using the $^1J_{\text{CH}}\text{-CT-CE-HSQC}$ experiment³² for the isotropic sample at 800 MHz (800 MHz) and 500 MHz (500 MHz), and oriented sample at 500 MHz (Phage), respectively. Due to coupling enhancement used in this NMR experiment, splittings correspond to $2 \times (J + D)$, and effects of CSA/dipole–dipole cross-correlation are reduced. Variation in splittings arises due to a variable residual dipolar contribution under direct field alignment (800 MHz) and in the presence of phage (Phage), as indicated by dashed lines. Residual dipolar couplings differ in both magnitude and sign for phage- and field-induced alignments.

an axially symmetric order tensor. As we demonstrate in this study, this degeneracy in the orientation of the C2-axis can also be overcome provided the measurement of two independent sets of residual dipolar couplings under two different alignment conditions.

The Measurement of Phage- and Field-Induced Residual Dipolar Couplings. For extended nucleic acids, partial alignment can be achieved by dissolving in ordered media,^{17,27} and also directly when under the influence of high magnetic fields.⁴² In Figure 2, we show representative spectra for one-bond ^1H – ^{13}C splittings measured between C8H8 nuclei in residue G8 using the $^1J_{\text{CH}}\text{-CT-CE-HSQC}$ experiment at 800 MHz (800 MHz), 500 MHz (500 MHz), and in the presence of phage at 500 MHz (Phage). The small differences between splittings measured at 500 and 800 MHz is attributed to a small dipolar coupling contribution arising from a very weak level of direct magnetic field alignment, while the larger differences between splittings measured at 500 MHz in the presence and absence of phage is attributed to a larger dipolar coupling contribution arising from a higher level of phage-induced molecular alignment. As shown in Figure 2 and listed in Table 1, field-induced dipolar couplings are not only reduced in size relative to phage-induced dipolar couplings, but they also exhibit a different relative magnitude and sign for different internuclear vectors. This is an indication that molecular alignment is different for the two cases and that phage- and field-induced dipolar couplings are independent measurements.

The order matrix approach that we use in this study relies on having five or more independent residual dipolar coupling measurements between nuclei in the bases of the G•(C–A) triad and G-tetrad motifs, respectively. While we have only measured six phage- and field-induced dipolar couplings in the G•(C–A) triad motif, the geometry of this sheared motif based on the NMR structure indicates a departure from a planar geometry, and hence, measured dipolar couplings should largely be independent. On the other hand, G-tetrads are likely to assume a more regular planar geometry. For an idealized G-tetrad motif

having a C4 axis of symmetry pointing along the normal to the guanine base planes, residues at opposing corners of the tetrad will have perfectly parallel internuclear vectors, and therefore identical dipolar coupling values, regardless of the mechanism of alignment. Moreover, a maximum of three independent dipolar couplings could be measured between base internuclear vectors that lie within the same plane. As shown in Table 1, $^1D_{\text{NH}}$ and $^1D_{\text{CH}}$ values are indeed more similar for residue pairs G1/G8 and G2/G9 than any other pairing combination, for both phage- and field-induced dipolar couplings, respectively. This is consistent with a directionality for the G-tetrad given by G1–G2–G8–G9, where G1/G8 and G2/G9 are at opposite corners of the G-tetrad (Figure 1c). However, there are also significant differences between dipolar couplings measured in opposing guanine residues, especially for the G1/G8 residue pair, and again, for both phage- and field-induced couplings (Table 1). This is strong evidence for a departure from an idealized G-tetrad geometry and that the eight dipolar couplings measured in the G-tetrad are also likely to be independent measurements. A small departure from an idealized geometry is indeed observed in the NOE-based NMR structure.³⁰

Determining the Relative Orientation of the G•(C–A) Triad and the G-Tetrad. One of the aims of this study is to demonstrate how the measurement of residual dipolar coupling can directly allow structure determination of monomeric units that belong to larger multimers, and for our application to the DNA homodimer d(G–G–G–T–T–C–A–G–G) quadruplex, the relative orientation of the G•(C–A) triad and G-tetrad motifs is a case in point. In Figure 3a, we show a Sauson–Flaumsted projection map⁴³ depicting principal orientational solutions for the G-tetrad (black dots) and G•(C–A) triad (green dots) determined using phage-induced residual dipolar couplings. The G-tetrad and G•(C–A) triad were assembled into a structure that is consistent with phage-induced dipolar couplings by superimposing the centers of the determined order tensor orientations depicted in Figure 3a. Since inversions about principal axes do not lead to changes in predicted dipolar coupling values, this led to four possible orientations of the G•(C–A) triad relative to the G-tetrad that are consistent with the phage-induced dipolar couplings.³⁶ Fixing the geometry of the G-tetrad, three additional relative orientations for the G•(C–A) triad were generated by rotating 180° about the principal x , y , and z directions, to yield a total of four relative G•(C–A) triad/G-tetrad orientations, TT_0 , TT_x , TT_y , and TT_z respectively.

As previously demonstrated, the orientational degeneracy that results from superimposing order tensor frames can be completely overcome by varying molecular alignment and acquiring two independent sets of dipolar couplings.³⁶ The four relative G•(C–A) triad/G-tetrad orientations (TT_0 , TT_x , TT_y , and TT_z) were therefore tested for consistency with field-induced dipolar couplings. Using the input coordinates from TT_0 , TT_x , TT_y , and TT_z , order tensors were calculated again, this time for the entire TT assembly using field-induced dipolar couplings. Only two of the four assemblies (TT_x and TT_0) produced order tensor solutions within our specified uncertainties (see materials and methods). The TT_z assembly was discarded because it could not simultaneously satisfy bond connectivity between G3/G2, G7/G8 and stacking between the G•(C–A) triad and G-tetrad. However, the fact that *two* and not *one* relative G•(C–A) triad/G-tetrad orientations were consistent with both phage- and field-induced dipolar couplings indicates that the two order tensors share a common principal axis direction; *this is exactly what one would expect in the presence of C2 molecular symmetry.*

(42) Kung, H. C.; Wang, K. Y.; Goljer, I.; Bolton, P. H. *J. Magn. Reson.* **1995**, *109*, 323–325.

(43) Bugayevskiy, L. M.; Snyder, J. P. *Map Projections: A Reference Manual*; Taylor & Francis: London, 1995.

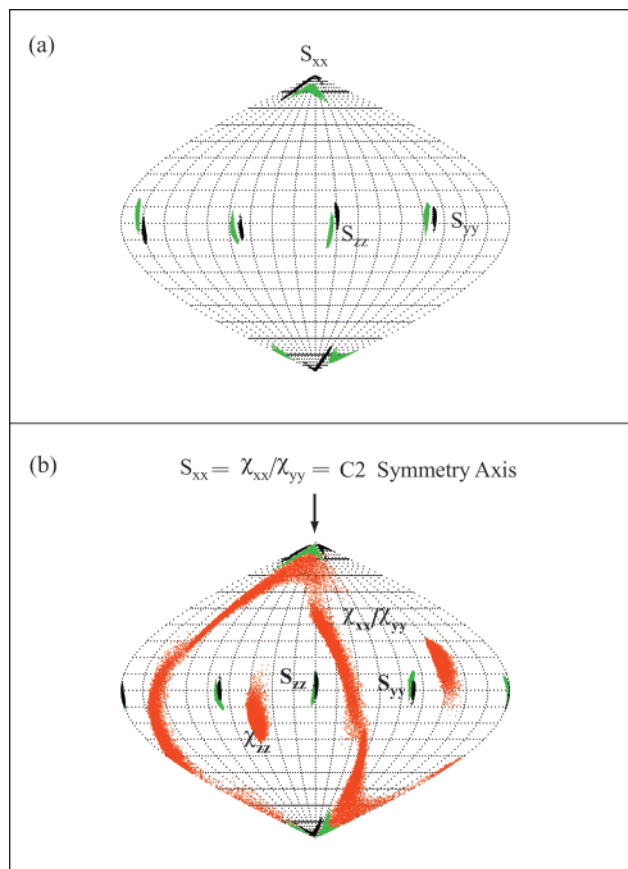


Figure 3. A Sauson–Flaumsted projection map⁴³ showing orientational solutions for determined order matrices. The Sauson–Flaumsted projection maps the surface of a unit sphere into a plane by converting latitude (ϕ) and longitude (λ) to Cartesian coordinates (x, y) via $y = \phi$ and $x = \lambda \cos \phi$. The horizontal lines of latitude run from -90° to 90° in 10° increments, while vertical curved lines of longitude run from -180° to 180° in 20° increments. Any point in this plot represents the orientation of a determined principal ordering axis relative to the molecular frame. The orientation of the three principal axes as well as corresponding inverted axes are shown. (a) Orientational solutions determined for phage-induced dipolar couplings (S_{xx} , S_{yy} , and S_{zz}) for the G*(C-A) triad (green dots) and G-tetrad (black dots), respectively. (b) Orientational solutions for the diamagnetic susceptibility tensor (χ_{xx} , χ_{yy} , χ_{zz}) determined using field-induced dipolar couplings and using the assembled G*(C-A) triad and G-tetrad (TT_0 , see text) as input coordinates (red dots). All orientational solutions are depicted relative to the determined principal axis system (PAS) of phage-induced dipolar couplings. Corresponding orientational solutions for the phage-induced alignment (S_{xx} , S_{yy} , and S_{zz}) are shown for the G*(C-A) triad (green dots) and G-tetrad (black dots), respectively. Orientational solutions for field- and phage-induced alignments overlap at only a *single* axis position, and this must therefore correspond to the invariable C2-axis of symmetry in the homodimer.

Determining the Direction of C2-Axis of Molecular Symmetry. Regardless of the nature of partial molecular alignment, the C2-axis of symmetry in a homodimer will always point along one of the principal directions of the order tensor or also uniformly along the principal x – y plane of an axially symmetric order tensor. The presence of a common principal direction of order between phage- and field-induced alignments can be verified by comparing order tensor orientational solutions for the two alignments relative to a common fragment frame. In Figure 3b, we depict the orientational solutions for order tensors determined using the field-induced residual dipolar couplings (black dots) and using the entire G*(C-A) triad/G-tetrad assembly (TT_0) as input coordinates. These solutions correspond

to the orientation of the diamagnetic susceptibility tensor of this DNA molecule, and χ_{ii} is used to make this distinction. For comparison, orientational solutions for phage-induced alignment are also shown using the same input coordinates, separately for the G-tetrad (red dots) and G*(C-A) triad (blue dots), respectively. As can be seen in Figure 3b, the orientations of the principal χ_{xx} and χ_{yy} axes lie almost uniformly within a plane, because the magnetic susceptibility tensor is close to axially symmetric, as one would expect for most DNA molecules.⁴⁴ Moreover, the orientation of χ_{zz} is tilted away from the phage-induced principal direction of order (S_{zz}) by at least 40° , and even though we have a large spread of orientational solutions for the magnetic susceptibility tensor, they overlap with orientational solutions from phage-induced alignment at only *one* axis position (Figure 3b). This axis also corresponds to the principal x direction, which explains why the TT_x assembly was consistent with both phage- and field-induced dipolar couplings. More significantly, because the orientation of the C2-axis of symmetry must always point along one of the principal directions of alignment, the x -axis must also unambiguously correspond to the C2-axis of symmetry. Interestingly, because the TT_x assembly is in fact generated by rotating the G*(C-A) triad 180° about the C2-axis, it is *not* a degenerate solution; rather, it corresponds to the orientation of the G-tetrad in one strand, relative to the G*(C-A) triad in the second strand in the homodimer.

The Topology of the DNA Homodimer. The principal aim of this study is to demonstrate how residual dipolar couplings can be used to determine the organization of monomeric units in homodimers. While superposition of order tensor frames allowed assembly of the G-tetrad and G*(C-A) triad within a monomeric unit, the orientation of principal directions of order can be used to determine the orientation of the C2-axis of symmetry and hence the relative orientation of the G-tetrad/G*(C-A) triad assembly relative to its equivalent C2 symmetry-related counterpart in the homodimer. The use of two independent sets of dipolar couplings allowed unambiguous determination of the C2-axis orientation.

The G*(C-A) triad/G-tetrad assembly (TT_0) was rotated about the determined C2-axis of symmetry to yield the relative orientation of the symmetry related counterpart (TT'_0) in the homodimer. While residual dipolar couplings do not inherently impose any translational constraints between monomeric units, *translation along a direction parallel to the C2-axis of symmetry is forbidden because it destroys C2 molecular symmetry in the homodimer*. In Figure 4, we show the topology of the DNA homodimer determined using residual dipolar couplings (Dipolar Fold). The structure of this DNA molecule has also previously been determined to very high precision ($\sim 0.4 \text{ \AA}$) using an unusually large number of observed NOE contacts as well as through hydrogen bond scalar coupling connectivities.³⁰ For comparison, this NOE-based fold (NOE Fold) is also shown in Figure 4; the two folds are in excellent agreement. The differences in the relative orientation of the G*(C-A) triad and G-tetrad in a contiguous monomeric unit is on average $\sim 12^\circ$, and as small as 5° within our orientational uncertainties (Figure 4a and 4b). The orientation of the C2-axis of symmetry deviates by as little as 5° , with deviations being about different axes for the G-tetrad (Figure 4a and c) and G*(C-A) triad (Figure 4a), respectively. Remarkably, while differences are very small, the average dipolar fold is more regular (Figure 4a and c).

(44) Tjandra, N.; Omichinski, J. G.; Gronenborn, A. M.; Clore, G. M.; Bax, A. *Nat. Struct. Biol.* **1997**, *4*, 732–738.

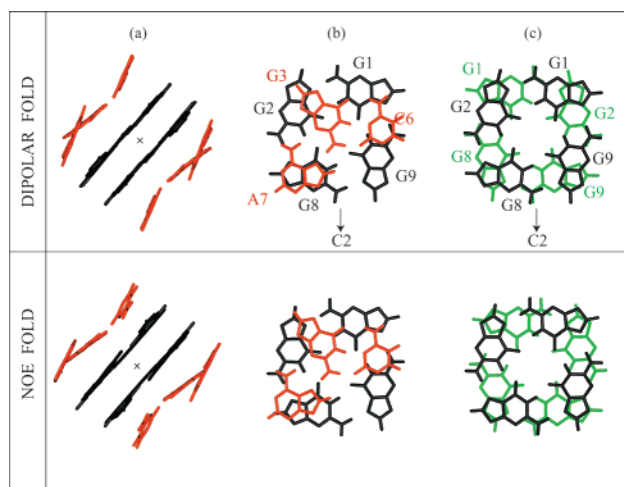


Figure 4. The folded topology of the dimeric d(G-G-G-T-T-C-A-G-G) quadruplex as determined using two sets of dipolar couplings (Dipolar Fold) and as previously determined by NMR using NOEs and through hydrogen-bond scalar connectivities (NOE Fold). (a) The overall C₂-symmetric topology of the DNA homodimer. Symmetry-related G•(C-A) triad and G-tetrad motifs are colored in red and black, respectively. The C₂ symmetry axis is superimposed for both folds and points out of the page as indicated by the symbol “×”. Motif ordering (i.e., G•(C-A) triad-G-tetrad-G-tetrad-G•(C-A) triad) in the dipolar fold is determined by insisting that G-tetrads cannot form within a single strand and by satisfying all bond connectivities. The two folds are in very close agreement, with the dipolar fold being slightly more regular. (b) Stacking of the G•(C-A) triad (in red) over the G-tetrad (in black). There are no translational constraints between these motifs in the dipolar fold, and hence the two folds should be compared from the point of view of relative motif orientations. The differences in the relative orientations of the G•(C-A) triad and the G-tetrad in the two folds is less than 12°. The direction of the C₂ symmetry axis is indicated using an arrow (C₂). (c) Stacking of the G-tetrad (in black) over a C₂-symmetry related G-tetrad (in green) in the DNA homodimer. Relative translation along the C₂-axis is prohibited because it breaks C₂ symmetry.

Concluding Remarks

The structure determination of multimers by NMR is a long-standing problem. As we have demonstrated in this study, residual dipolar couplings can play an important role in this determination. Using an order matrix approach, we were able to directly determine the relative orientation of structural motifs within a monomeric unit, even in the presence of inter- and intrastrand NOE ambiguity. More significantly, the position of the C₂-axis relative to individual monomeric units was very well determined using two independent sets of dipolar data, which in turn lead to accurate determination of relative monomer orientation in the homodimer. Obtaining such decisive constraints on long-range aspects of the molecular structure is critical in extended DNA molecules, especially for more complex, higher-order folds having more than one symmetry axis, where several DNA topologies are often consistent with measured NOE contacts. The presented approach can readily be extended to molecular architectures having three orthogonal C₂ symmetry axes, in which case all three principal directions of the determined order tensor will point along the three C₂ symmetry axes. The present approach can also be applied in the structure determination of protein homodimers, where establishing the spatial orientation of known secondary structural elements is often complicated by ambiguous intra- and inter-monomer side-chain NOE contacts.²³

Our presented study relied on being able to modulate molecular alignment to allow measurement of two independent

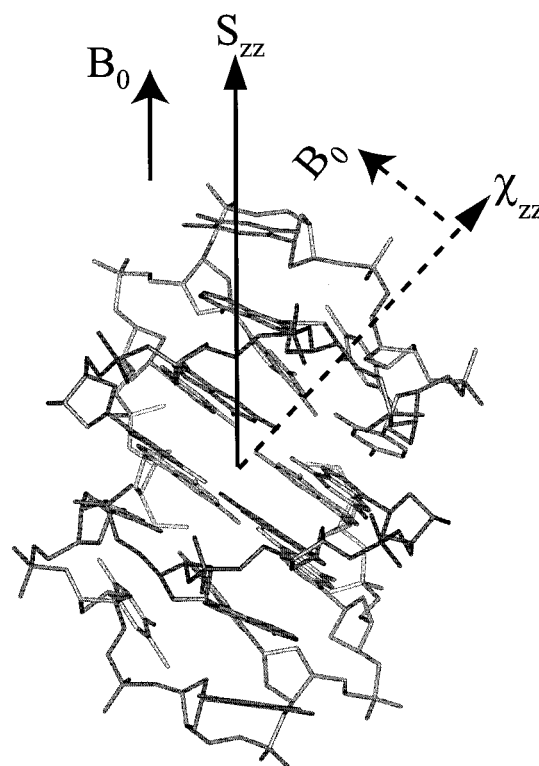


Figure 5. Orientation of the principal axis of order (S_{zz}) and magnetic susceptibility (χ_{zz}) determined using phage- and field-induced dipolar couplings, respectively. Orientations are shown relative to the NOE-based NMR structure.³⁰ The principal direction of phage-induced order S_{zz} points almost perfectly along the long axis of the molecule, while the direction of χ_{zz} is close to parallel to the base-plane normals. These two orientations differ by $\sim 45^\circ$. S_{zz} also has a positive value for phage-induced alignment, indicating alignment with the long axis of the molecule pointing parallel to the magnetic field, while χ_{zz} has a negative value, indicating that alignment is perpendicular to the field. Ordered media and field-induced alignment can provide independent sets of dipolar coupling data in nucleic acids.

sets of dipolar couplings. For protein systems, alignment in ordered media appears to result from an interplay of steric collisions⁴⁵ and charge–charge interactions;⁴⁶ a feature which readily allows variation of molecular alignment by simply changing the charge composition of the used ordered medium.^{36,47} However, because linear DNA molecules tend to have a more uniform distribution of charge and greater regularity in structure, it can be anticipated that modulating molecular alignment by varying the ordered medium, particularly its orientation, will not be easy. An alternative that has been used in this study is direct magnetic field alignment. Even though field-induced dipolar couplings were small in magnitude relative to uncertainties, and hence not used as primary data in this work, they were sufficient to overcome orientational degeneracies. As shown in Figure 5, the orientation of the principal S_{zz} axis in the phage-induced alignment is almost perfectly along the long axis of the molecule, while the orientation of principal axis of the magnetic susceptibility tensor (χ_{zz}) is almost parallel to the normal of the base planes, and this direction deviates from the long axis by at least $\sim 40^\circ$. This noncollinearity of base normals and long axes requires substantiation in other nucleic acids, but direct magnetic field alignment should always be a viable option

(45) Zweckstetter, M.; Bax, A. *J. Am. Chem. Soc.* **2000**, *122*, 3791–3792.

(46) Sass, J.; Cordier, F.; Hoffmann, A.; Cousin, A.; Omichinski, J. G.; Lowen, H.; Grzesiek, S. *J. Am. Chem. Soc.* **1999**, *121*, 2047–2055.

(47) Ramirez, B. E.; Bax, A. *J. Am. Chem. Soc.* **1998**, *120*, 9106–9107.

for supplementing an independent set of dipolar couplings to data acquired using an ordered medium.

Despite much anticipation about the utility of residual dipolar coupling methodology in the structure determination of extended nucleic acids,^{15,17} and despite several reports documenting the measurement of residual dipolar couplings in nucleic acids,^{18,48,49} only two examples reporting a direct utility in structure determination have so far appeared in the literature.^{26,27} One of the factors that can complicate analysis of residual dipolar couplings in nucleic acids, that has recently been highlighted in a recent study by Bax and co-workers, is the small number of independent residual dipolar couplings that can be measured.²⁷ As shown in this study, one way to alleviate this situation is to supplement a single set of residual dipolar coupling measurements with an independent set acquired under a different alignment condition, as well as other sources of information to help define local geometry. For applications to nucleic acids, observation of trans-hydrogen bond scalar couplings is a powerful and simple approach for characterizing base paired alignments, as has now been demonstrated in a number of studies.^{9,40,50–54} Moreover, motifs such as G-tetrads (possibly hexads⁴¹) are likely to adopt known alignment geometries.⁴

(48) Hansen, M. R.; Rance, M.; Pardi, A. *J. Am. Chem. Soc.* **1998**, *120*, 11210–11211.

(49) Clore, G. M.; Murphy, E. C.; Gronenborn, A. M.; Bax, A. *J. Magn. Reson.* **1998**, *134*, 164–167.

(50) Majumdar, A.; Kettani, A.; Skripkin, E. *J. Biomol. NMR* **1999**, *14*, 67–70.

(51) Dingley, A. J.; Masse, J. E.; Peterson, R. D.; Barfield, M.; Feigon, J.; Grzesiek, S. *J. Am. Chem. Soc.* **1999**, *121*, 6019–6027.

(52) Wohnert, J.; Dingley, A. J.; Stoldt, M.; Grolach, M.; Grzesiek, S.; Brown, L. R. *Nucleic Acids Res.* **1999**, *27*, 3104–3110.

(53) Hennig, M.; Williamson, J. R. *Nucleic Acids Res.* **2000**, *28*, 1585–1593.

While the NMR-derived G-tetrad geometry slightly deviates from a typical idealized geometry, similar order tensor orientational solutions are obtained when using the two input geometries, except that dipolar coupling uncertainties had to be further raised for the idealized geometry (by ~20%) before order tensor solutions could be determined. Another complication that can arise in the analysis of dipolar couplings in nucleic acids is conformational flexibility. In this study, we deliberately did not include dipolar couplings measured between nuclei in the ribose sugar in our analysis. This was partly because including sugar rings to our chosen fragments requires a priori local information that is not generally available or readily accessible (for example the angle χ). However, one should also be cautious about including dipolar data in conformationally flexible sugar rings during a structural analysis. As has recently been examined extensively,³⁷ internal motions affect dipolar couplings in an intricate manner, and when not properly accounted for, this can lead to erroneous results in structure calculation. While the order tensor approach that we use in this study is in fact highly tolerant to collective fragment motions, extensive internal motions within a fragment can be more complicated.³⁷

Acknowledgment. We thank Dr. B. Agazadeh for preparing the phage medium, Dr. E. R. P. Zuiderweg for 800 MHz time at the University of Michigan, and Dr. J. R. Tolman for useful comments on the manuscript. This work was supported by a grant from the NIH GM-34504 to D. J. P.

JA003379Y

(54) Dingley, A. J.; Masse, J. E.; Feigon, J.; Grzesiek, S. *J. Biomol. NMR* **2000**, *16*, 279–289 studies of RNA.